Regular Article

ANALYTICAL AND BIOANALYTICAL CHEMISTRY RESEARCH

Published by the Iranian Chemical Society

Anal. Bioanal. Chem. Res., Vol. 8, No. 4, 467-480, September 2021.

Fabrication of a Novel Phenolic Compound Biosensor Using Laccase Enzyme and Metal-organic Coordination Polymers

Doaa Jalil Abosadeh[a], Soheila Kashanian[b,c,*], Maryam Nazari[a] and Fatemeh Parnianchi[a]

[a]*Faculty of Chemistry, Razi University, Kermanshah, Iran*

[b]*Faculty of Chemistry, Sensor and Biosensor Research Center (SBRC) & Nanoscience and Nanotechnology Research Center (NNRC), Razi University, Kermanshah, Iran*

[c]*Nano Drug Delivery Research Center, Kermanshah University of Medical Sciences, Kermanshah, Iran*

(Received 26 December 2020 Accepted 30 May 2021)

Hydroquinone (HQ) sensitive electrochemical biosensing was performed using new nanocomposites of carboxylated graphene (GrCOOH) embedded in metal-organic coordination polymers (MOCPs) as efficient matrices for laccase (Lac) immobilization. GrCOOH nanosheets were used to pre-adsorbotion of $HAuCl_4$ and acted as anchor sites. They help to form MOCPs and more coordinates between gold ions and 4-aminothiophenol (4-ATP) ligand. According to the Tafel plot, the mechanism was diffusion for HQ redox reactions on the proposed modified electrode surface and an electron process was in the rate-determining stage. It was concluded that this redox reaction was involved the same number of protons and electrons. The construction of GrCOOH-MOCPs one-pot entrapped Lac exhibited enhanced redox currents over MOCPs for HQ electrochemical oxidation and reduction and enhanced sensitivity and low detection limit (1.70 μM), being superior to other Lac biosensors. Furthermore, this biosensor was tested in real samples and demonstrated acceptable recoveries in real water samples, and showed a good stability for one week.

Keywords: Laccase, Biosensor, Metal-organic coordination polymers, Hydroquinone, Graphene

INTRODUCTION

Biosensors are becoming important in a wide range of analyses. Numerous biosensor types have been developed, including electrochemical, piezo-electric, colorimetric, mechanical, and optical biosensors [1]. Cells, tissue slices, and enzymes that produce chemical or electroactive molecules, when recognizing and reacting with the target analyte, can be used in biosensors fabrication and display a number of features including reusability, easily regeneration, and rapid analysis [2].

When natural organic compounds are broken down, the phenolic compounds produced act as antioxidants with anticancer activity [3]. Though, some phenolic compounds are common pollutants, produced from chemical industrial activities, which can penetrate to natural waters through the industries effluents such as petrochemicals, pharmaceuticals, coal refineries, pulp, paints, textiles and resin factories [4,5]. Although chromatographic and spectrophotometric systems are the most general techniques for phenolic compounds detection, the focus has been mainly on bioanalytical instruments such as biosensors due to their ability in highly accurate measurements at trace levels [6]. Electrochemical biosensors offer advantages including rapidity, simplicity, ease miniaturization, and high sensitivity and selectivity [7].

Due to particular and peculiar properties of enzymatic biosensors, their applications have enhanced over time. Up to now, several enzymatic biosensor studies have been conducted to detect phenolic compounds based on several enzymes such as tyrosinase [8-10], horseradish peroxidase (HRP) [11,12] and laccase (Lac) [13-19]. Lac (benzenediol:

*Corresponding author. E-mail: kashanian_s@yahoo.com

oxygen oxidoreductase, EC 1.10.3.2) belongs to a group of polyphenol oxidases providing some special advantages over other enzymes, which can be considered as a strong biological sensor [20,21]. It is usually called multicopper oxidase due to the presence of copper atoms in the catalytic center [22]. It catalyzes O_2 reduction to H_2O accompanied by substrate oxidation, typically a *p*-dihydroxy phenol or another phenolic compound. Lac is an important enzyme owing to oxidizing both the toxic and nontoxic substrates and it has a variety of substrates [23].

Various methods were reported for Lac immobilization. Recently, several immobilization strategies have been used including adsorption [24-26], cross linking [27-29], layer by layer assembly [30,31], sol-gel entrapment [32-34] and electropolymerization [35].

Lac biosensors have been studying for the past 20 years. Malinowski *et al.* (2020) developed an electrochemical Lac-based biosensor using a Corona SPP (Soft Plasma Polymerization) technique for fabrication of the Lac sensing layer. They used it to detect dihydroxybenzene isomers (catechol, hydroquinone and resorcinol) in real water samples [4]. Zhang *et al*., (2020) fabricated a Lac biosensor for detection of catechol based on a nanocomposite of gold-nanoparticles (AuNPs) and MoS_2 nanosheets [36].

Metal-organic coordination polymers (MOCPs), also known as metal-organic frameworks (MOF), [37] have been used in different fields such as drug release/delivery, catalysis, chemical separations, gas storage, sensor and biosensors due to their outstanding chemical and physical properties [38]. MOCPs and nanomaterials such as carbon-nanotube (CNT), graphene (Gr) and AuNPs still leave room for biosensor improvement. Recently, MOCPs have been used as greatly efficient enzymatic immobilization matrices [39]. They contain coordinated ligands and are linked to metal ions, that conformed an infinite array with an automatically formation process that is called "self-assembly process" [40].

4-Aminothiphenol (4-ATP) is one of the organic compounds used to prepare surfaces in sensor applications. To prepare electro-active supports, diverse nanoparticles such as quantum dots [41], graphene oxide [42] and AuNPs [43] were covered with 4-ATP using its dropping/electro-polymerization on the nanomaterial surfaces [44].

Gr, obtained from graphite, is composed of carbon atoms in monolayer arrayments packed into a dense structure of honeycomb crystal. Since 2004, Gr has been used for enzyme immobilization and biosensor fabrication due to its high specific surface area and presenting extraordinary electron transport property [45]. The synthesis of carboxylated graphene (GrCOOH)/MOF composites was demonstrated to be an effective way for improvement of MOF properties [46].

In this study, a new nanocomposite of GrCOOH and MOCPs was considered as an efficient matrix for Lac immobilization and electrochemical biosensing of hydroquinone (HQ) (as an example of phenolic compound) with high sensitivity and selectivity.

EXPERIMENTAL

Reagents and Materials

Dimethylformamide (DMF) and HQ were bought from Merck. Lac, $HAuCl_4$, and 4-amino-thiophenol (4-ATP) were purchased from Sigma-Aldrich. Sodium dihydrogen phosphate (NaH_2PO_4) and citric acid were obtained from BDH. All the other materials were purchased from Merck.

Instrumentation

To analyze the nanostructures, and investigation of surface morphology, Quanta 450 scanning electron microscope (Fei Company, USA) was used to obtain the scanning electron microscopy (SEM) images. The specimens should be coated with gold before scanning by the probe of microscope. Using this characterization technique, the shape, diameter, thickness, length and orientation of nanostructures could be investigated. The images were produced by scanning the sample with a focused beam of electrons. The interaction of electrons with the atoms available in the sample creates several signals which can be observed. These signals provide information about the composition and surface topography. For more accurate resolution (better than 1 nanometer) SEM could be also employed. Also, Fourier transform infrared (FTIR) spectroscopy (Bruker FTIR-6000 spectrometer) was applied to investigate functional groups and MOCP synthesis confirmation using KBr pellets in a wavenumber range of

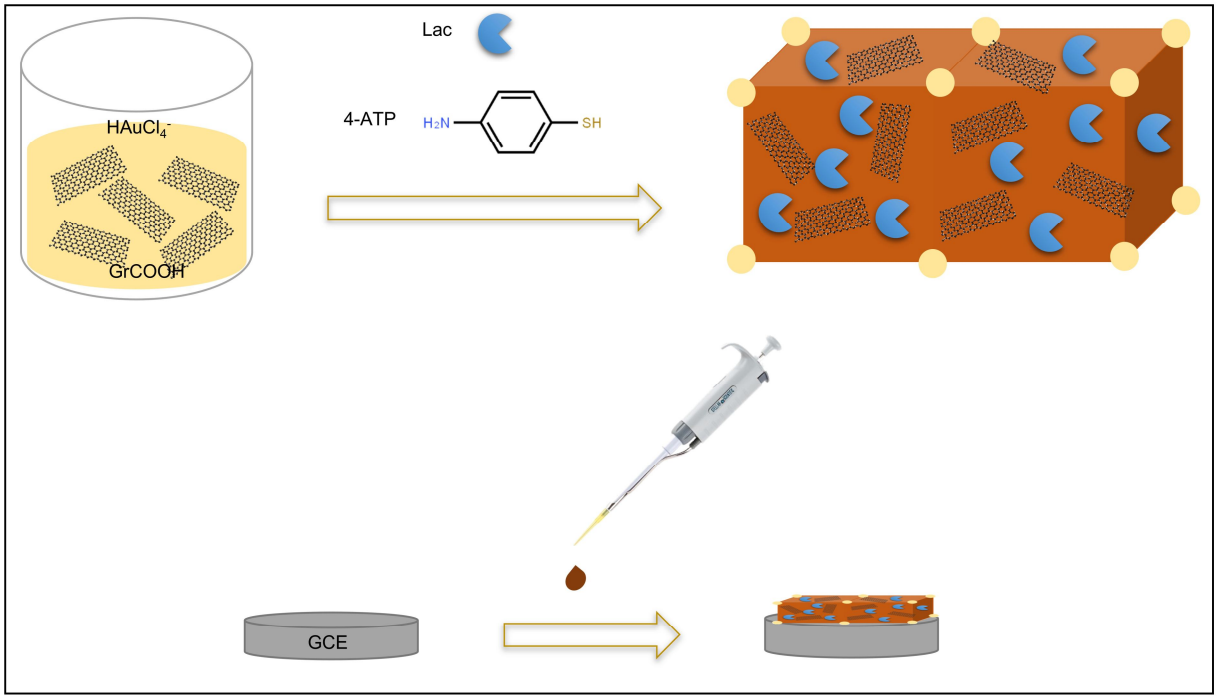

Scheme 1

400-4000 cm^{-1}.

In this research, voltammetry technique was used to study the biosensing under the presence and absence of HQ. All electrochemical experimentations were conducted using an electroanalyzer of SAMA 500 that was controlled by a computer. It equipped three-electrodes: calomel electrode as a reference electrode, the bare and modified GCEs as working electrodes, and platinum electrode as an assisting electrode. All of the electrodes were prepared from Azar electrode. The cyclic voltammograms were recorded from -0.5 to 1.2 V at a scan rate of 0.1 V s^{-1} for this biosensor with and without HQ, respectively. To investigate the biosensor, phosphate buffer solution (PB) with various pH values embraced the system. The pH value is a key factor in the biochemical reaction which takes place at the electrode-solution interface. Since the enzymes are active in a particular pH range, it is significant to optimize the pH to achieve the best enzyme catalytic response. Accordingly, the present analysis assesses the effect of pH between 4.0 and 9.0 on the activity of the GCE modified with composite containing Lac. After selection of the best pH, the other voltammetry experiments were done in the optimized pH.

MOCPs Preparation and Enzyme Electrodes Fabrication

In the MOCP cases, 300 µl of 1 mg ml^{-1} GrCOOH aqueous suspension and 60 µl $HAuCl_4$ (0.05 M) were added to 1 ml PB (pH 6) and it was incubated under stirring for 2 h, then 200 µl of Lac (4 mg ml^{-1}) mixture and 4-ATP (1 mg ml^{-1}) were added. The mixture was stirred for 10 min to stimulate reaction and to obtain MOCP (without GrCOOH and Lac), MOCP-GrCOOH (without Lac), or MOCP-GrCOOH-Lac composites. Hence, the composite suspensions were centrifuged, and the precipitants were washed three times, and then dispersed in water (200 µl) [39]. To fabricate the electrode, GCE was polished with fine sandpaper and alumina dough followed by rinsing with ultra-pure water, after that the electrode surface was covered with 7 µl of MOCP, MOCP-GrCOOH, or MOCP-GrCOOH-Lac, and then allowed to dry at room temperature. The biological sensor was stored in the refrigerator at 4 °C when not in use. Scheme 1 shows the

composite preparation and electrode modification.

RESULTS AND DISCUSSION

Modified Electrode Characterization

Scanning electron microscopy (SEM) studies. According to Fig. 1, surface morphological analyses of MOCP-GrCOOH/GCE and MOCP-GrCOOH-Lac/GCE were monitored by SEM images. It is strongly concluded that the MOCP is favorably deposited on the GCE. The MOCP-GrCOOH increased the porosity and surface area that can facilitate the transferring of electrons on the electrode surface. Figures 1b and 1d demonstrate the Lac immobilization on the modified GCE that the spaces were occupied and the porosity was reduced.

Fourier Transform Infrared (FTIR) Spectroscopy

Figure 2 displays the FTIR spectrum of MOCP in comparison with the spectrum of 4-ATP. Based on the spectrum of MOCP, 3440 and 3325 cm^{-1}, wavelengths belong to the characteristic bands of the NH_2 group. Concerning the spectrum of MOCP compared to the spectrum of 4-ATP, it can be realized that the SH stretching vibration (2553 cm^{-1}) has been vanished and at 937 cm^{-1} a new absorption peak is appeared for MOCP, which is attributed to the Au-S bond vibrations [39]. Consequently, the S-Au bond formation can be concluded due to significant changes in characteristics of many thiol vibrations. Furthermore, some of the vibrational intensities in the fingerprint area have been diminished or vanished. Hence, the formation of bond between AuNPs surface and 4-ATP can be confirmed.

Voltametric Response

Cyclic voltammetry (CV) is an electrochemical technique to study the kinetics of redox reactions and conducting characteristics at electrodes under closely monitored states. CV contains plotting current that flows as a function of the employed potential. The CVs of Lac-based biosensor were inspected in PB under the potentials ranging from -0.5 to 0.8 V for the optimization of pH, and the investigation of scan rate effect in the absence of HQ and -0.5 to 1.2 V at pH 6 for other electrochemical experiments including the investigation of scan rate effect in the presence of HQ, investigation of interferences effect, obtaining a calibration curve, and real sample observations. Also, to compare modified electrodes in the solution containing $Fe(CN)_6^{3-/4-}$, the potential range of -0.5 to 1.2 V and the scan rate of 0.1 V s^{-1} were applied.

Electrochemical Behavior of Modified Electrodes in the Presence of Redox Probe and Hydroquinone

The current-potential curves for modified electrodes in KCl solution containing $Fe(CN)_6^{3-/4-}$ are shown in Fig. 3a. In addition, Table 1 indicates the redox currents and potential amounts. E_p^a is considered as the anodic peak potential, and E_p^c is considered as the cathodic peak potential. It shows that the MOCP-GrCOOH/GCE has the highest redox currents due to the large surface area of GrCOOH and its porous structure to transfer the electron of $Fe(CN)_6^{3-/4-}$ redox probe.

The Lac immobilized electrode was verified as a biosensor to diagnose HQ. The determination of HQ was performed in the PB at pH 6.0. The current-potential curves for modified electrodes in PB at pH 6 in the presence of HQ are shown in Fig. 3b. According to this Figure, there are two redox peak potentials for HQ on the surface of GCE. Here, E_p^a is regarded as HQ oxidation to p-quinone and E_p^c is regarded as p-quinone reduction to HQ. In Table 2, the data for E_p^a and E_p^c and also i_p^a and i_p^c are shown as well. The Lac-based electrode (MOCP-GrCOOH-Lac/GCE) has the highest catalytic capacity for HQ oxidation compared to the other modified electrodes. It may also be assigned to the larger specific surface area through which more Lac enzymes can be loaded to engage in catalytic reaction.

Biosensor pH Optimization

The pH has a high impact on enzymatic reactions. Enzymes have a maximum speed of reactions and activity at optimal pH. Accordingly, the current study has investigated pH effect between 4.0 and 9.0 on the response of MOCP-GrCOOH-Lac. Optimal pH for Lac activity relies on the sort of substrates [47]. In the case of phenols, fungal Lac has typically optimal activity in the pH range of 3.0-7.0 [48]. As a preceding data, the activity of Lac enzyme happens in an acidic system. The optimum pH was examined for MOCP-GrCOOH-Lac/GCE biosensor. To evaluate, it was incorporated in buffer solutions with

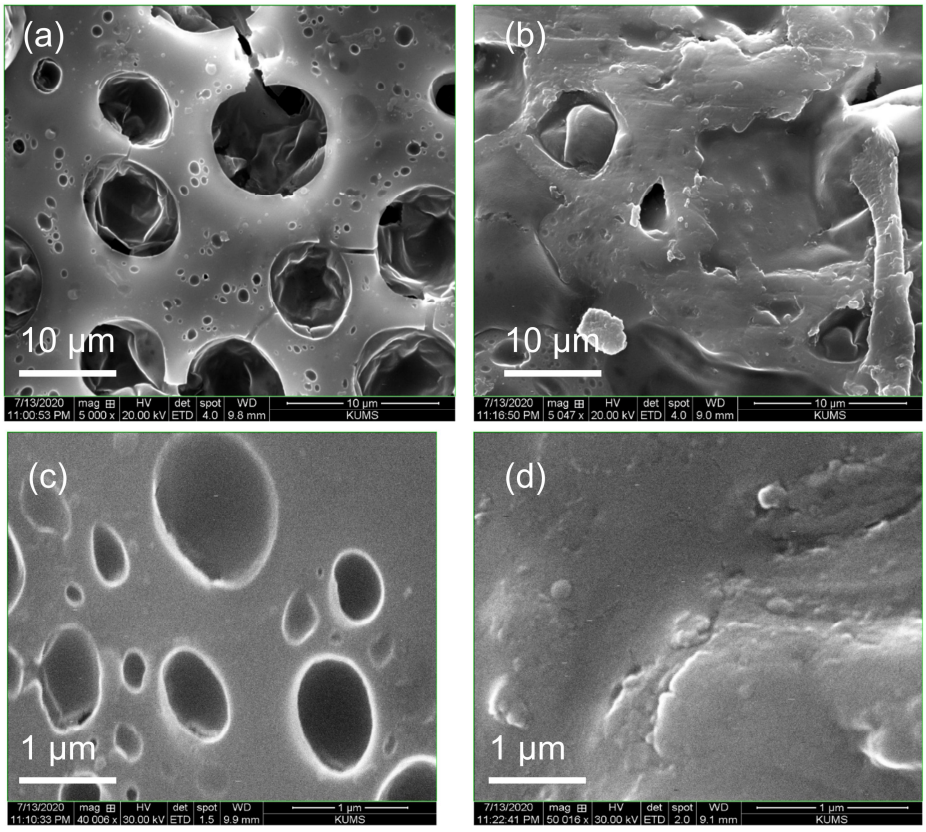

Fig. 1. SEM images of the electrode surfaces modified with MOCP-GrCOOH/GCE (a, c) and MOCP-GrCOOH-Lac/GCE (b, d).

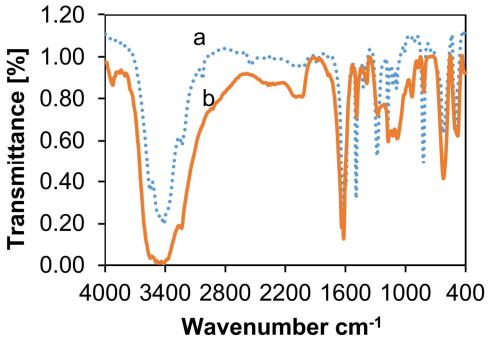

Fig. 2. Infrared absorption spectra of 4-ATP (a), and MOCP (b).

different pH values (4.0 to 9.0) (Fig. 4a). Relatively, the response of the biosensor is expanded by increasing the current. The Lac biosensor has higher currents in PB at pH 6. The current was declined in more acidic and basic media as shown in Fig. 4b. The optimum pH was selected to be 6 and it is in agreement with the previous experiments

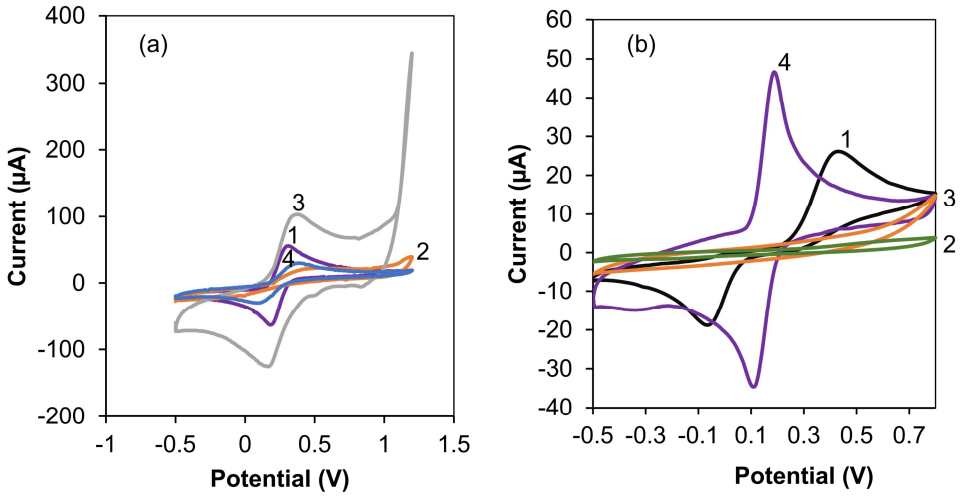

Fig. 3. CVs in 0.1 M KCl containing 5 mM $K_3(CN)_6/K_4(CN)_6$ (a) and CVs in PB pH 6 containing 1.0×10^{-3} M HQ (b). 1) GCE, (2) MOCP/GCE, (3) MOCP-GrCOOH/GCE and (4) MOCP-GrCOOH-Lac. Scan rate: 0.1 V s^{-1}.

Table 1. Voltammetric Data for (a) GCE, (b) MOCP/GCE, (c) MOCP-GrCOOH/GCE and (d) MOCP-GrCOOH-Lac/GCE in 0.1 M KCl Containing $K_3(CN)_6/K_4(CN)_6$

Electrode	E_p^a (V)	i_p^a (µA)	E_p^c (V)	i_p^c (µA)	$E_p^a - E_p^c$ (V)
(a) GCE	0.428	19.28	-0.064	-16.22	0.364
(b) MOCP	-0.14	0.256	-0.168	--0.16	-0.028
(c) MOCP-GrCOOH	-0.235	0.811	-0.103	-0.312	-0.132
(d) MOCP-GrCOOH-Lac	0.186	39.58	0.109	-32.67	0.077

[49]. As a result, pH 6 was used for further determination of HQ at the MOCP-GrCOOH-Lac/GCE.

Figure 4c displays clearly the linearly changing of formal potential ($E^{0'} = (E_p^a + E_p^c)/2$) of Lac biosensor *versus* pHs. The linear regression equation was found as $E^{0'} = -0.0518$ pH + 0.466 with the correlation coefficient of 0.99. It can be concluded that pH affects this redox reaction and the same number of protons and electrons can participate in the reaction.

Effect of Scan Rate

One of the most pivotal parameters is the evaluation of the scan rate effect on the anodic and cathodic currents and potentials, which affects the redox features of the substrates in the voltammetry techniques. To investigate the effect of scan rate on biosensor response, CV was performed employing PB (pH 6) in the absence and presence of HQ in a series of scan rate values (in the range of 0.02-1 V s^{-1}).

Effect of Scan Rate onto MOCP-GrCOOH-Lac without HQ

The voltammograms are given in Fig. 5a. The oxidation and reduction peak currents increase with rising the scan rates and there is a linear relation between the peak current and scan rate, which has correlation coefficients of 0.99 and 0.97 for both cathodic and anodic currents, respectively

Table 2. Voltammetric Data for (a) GCE, (b) MOCP (c) MOCP-GrCOOH/GCE and (d) MOCP-GrCOOH-Lac/GCE in PB pH 6 Containing 1.0×10^{-3} M HQ

Electrode	E_p^a (V)	i_p^a (µA)	E_p^c (V)	i_p^c (µA)	$E_p^a - E_p^c$ (V)
(a) GCE	0.320	59.83	0.168	-54.74	0.152
(b) MOCP	0.428	13.57	-0.005	-4.245	0.423
(c) MOCP-GrCOOH	0.345	79.93	0.159	-84.33	0.186
(d) MOCP-GrCOOH-Lac	0.386	24.79	0.096	-21.55	0.29

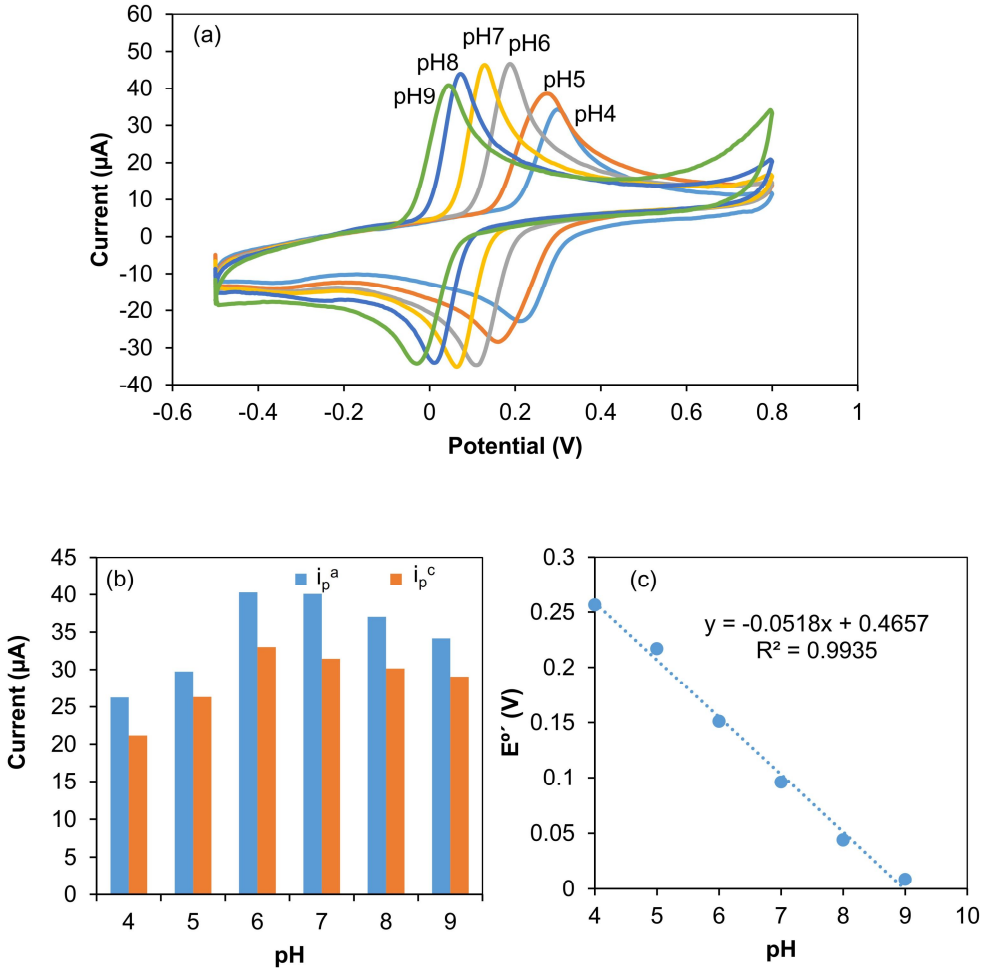

Fig. 4. CVs of pH effect on the current responses of HQ oxidation and reduction for MOCP-GrCOOH-Lac/GCE in 0.1 M PB at pH 6 containing 1.0×10^{-3} M HQ. Scan rate: 0.1 V s^{-1} (a). Anodic and cathodic currents *versus* different pHs (b). The plot of formal potential *versus* various pHs (c).

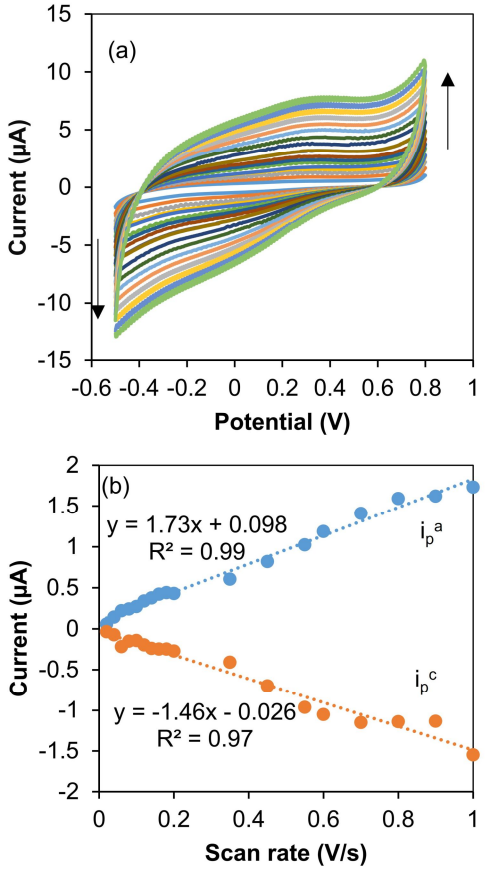

Fig. 5. CVs of MOCP-GrCOOH-Lac/GCE in different scan rates in 0.1 M PB at pH 6 (a). The relationship between anodic and cathodic peak currents with scan rate (b).

(Fig. 5b); this behavior contributes to the adsorption of the substrate onto the surface of the electrode [50].

Effect of Scan Rate onto MOCP-GrCOOH-Lac/GCE with HQ

The voltammograms of HQ onto the MOCP-GrCOOH-Lac/GCE are given in Fig. 6a. The oxidation and reduction peaks enhanced with increasing the scan rates (Fig. 6b) and a linear relationship was found between the peak current and the square of scan rate, with a correlation coefficient of 0.959 and 0.961 for both anodic and cathodic currents (Fig. 6c), leading to diffusion of the substrate to the electrode surface [50].

As the scan rates grow up, the anodic peak potential moved to the positive potential direction to some extent, whereas the cathodic peak potential shifted moderately to the negative potential direction (Fig. 6d) which indicated a quasi-reversible electrochemical reaction process [36]. The detected behavior relies upon transfer coefficient (α) and the standard heterogeneous rate constant (k_s) [51].

Figure 6d shows the anodic peak potential (E_p^a) and cathodic peak potential (E_p^c) relationship with the logarithm of the scan rate (log*v*) for this biosensor in 0.1 M PB (pH 6) containing 1 mM of HQ changed linearly *versus* logυ with a linear regression equation of E_p^c = -0.044 log*v* + 0.069; R^2 = 0.97 and E_p^a = 0.036 log*v* + 0.22; R^2 = 0.96 in the range of 0.02-1 V s^{-1}.

The Tafel plot is an effective way to investigate the kinetic parameters when the mechanism is diffusion [52]. Using the data collected from the growing part of the

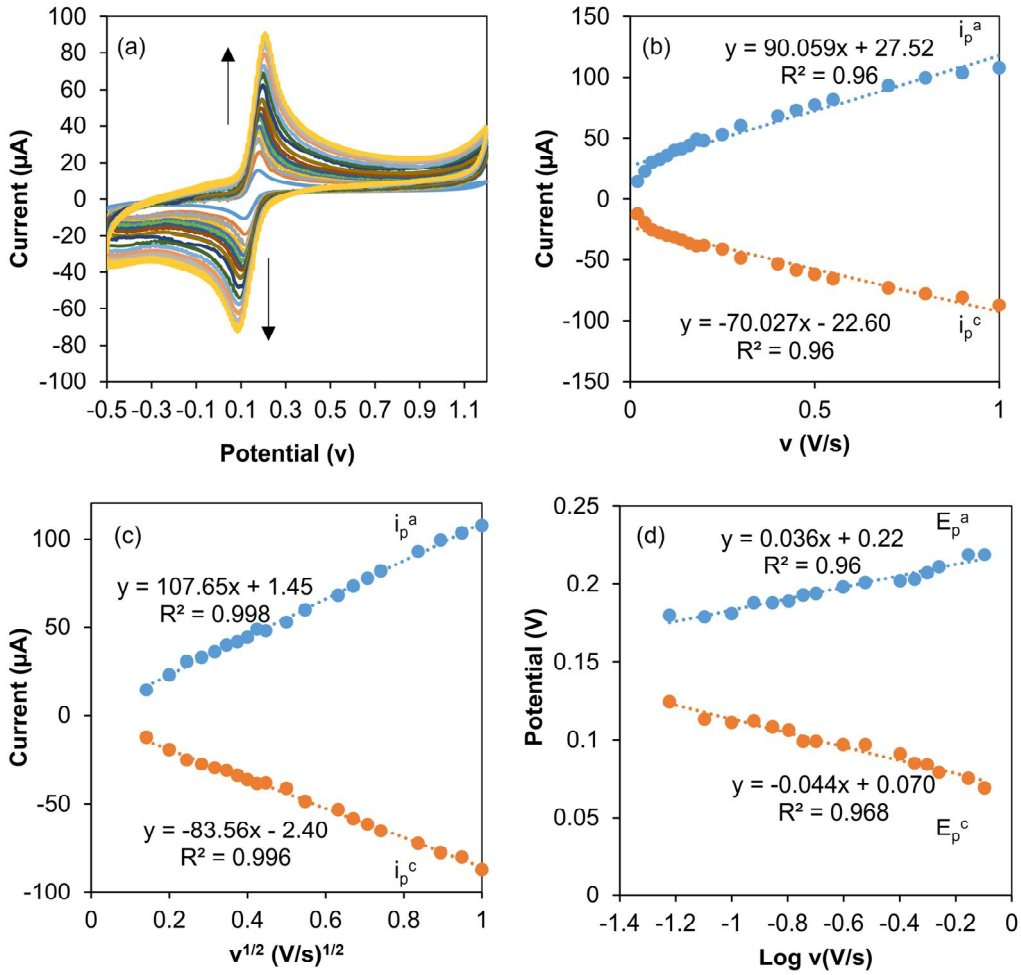

Fig. 6. CVs of MOCP-GrCOOH-Lac/GCE in different scan rates in 0.1 M PB at pH 6 containing 1.0×10^{-3} M HQ (a). The relationship between the anodic and cathodic peak currents with scan rate (b). The relationship between the anodic and cathodic peak currents with the square of scan rate (c). Dependence of peak potentials *versus* scan rate in logarithmic scale (d).

current-voltage curve recorded at a scan rate of 20 mV s^{-1}, a Tafel plot was achieved (Fig. 7). The slope of the drawn plot is equal to n(1 - α)F/2.3RT or 19.307 decade/V, the charge transfer coefficient (α), calculated from the slope was detected to be 0.43, that is the indication of involving an electron process in the rate-determining stage [51,53,54]. According to the pH effect data and Tofel plot, the number of both electrons and protons can be considered as two [55]; hence, Lac catalyzes the oxidation of HQ into 1,4-benzoquinone (1,4 BQ), which is followed by reduction of molecular oxygen, as described by the following reactions [56]:

$$HQ + Lac\ (oxy) \rightarrow 1,4\ BQ + Lac\ (deoxy) + 2H^+ + 2e \quad (1)$$

$$Lac\ (deoxy) + O_2 + 4H^+ \rightarrow Lac\ (oxy) + 2H_2O \quad (2)$$

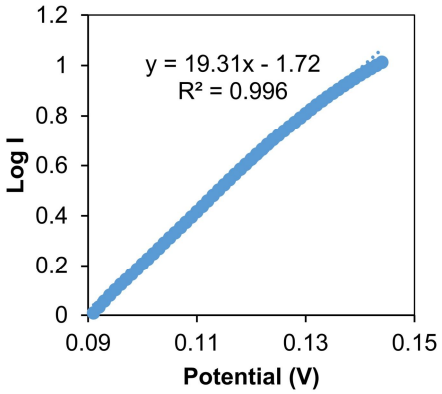

Fig. 7. Tafel plot derived from the rising part of voltammograms recorded at a scan rate 20 mV s^{-1}.

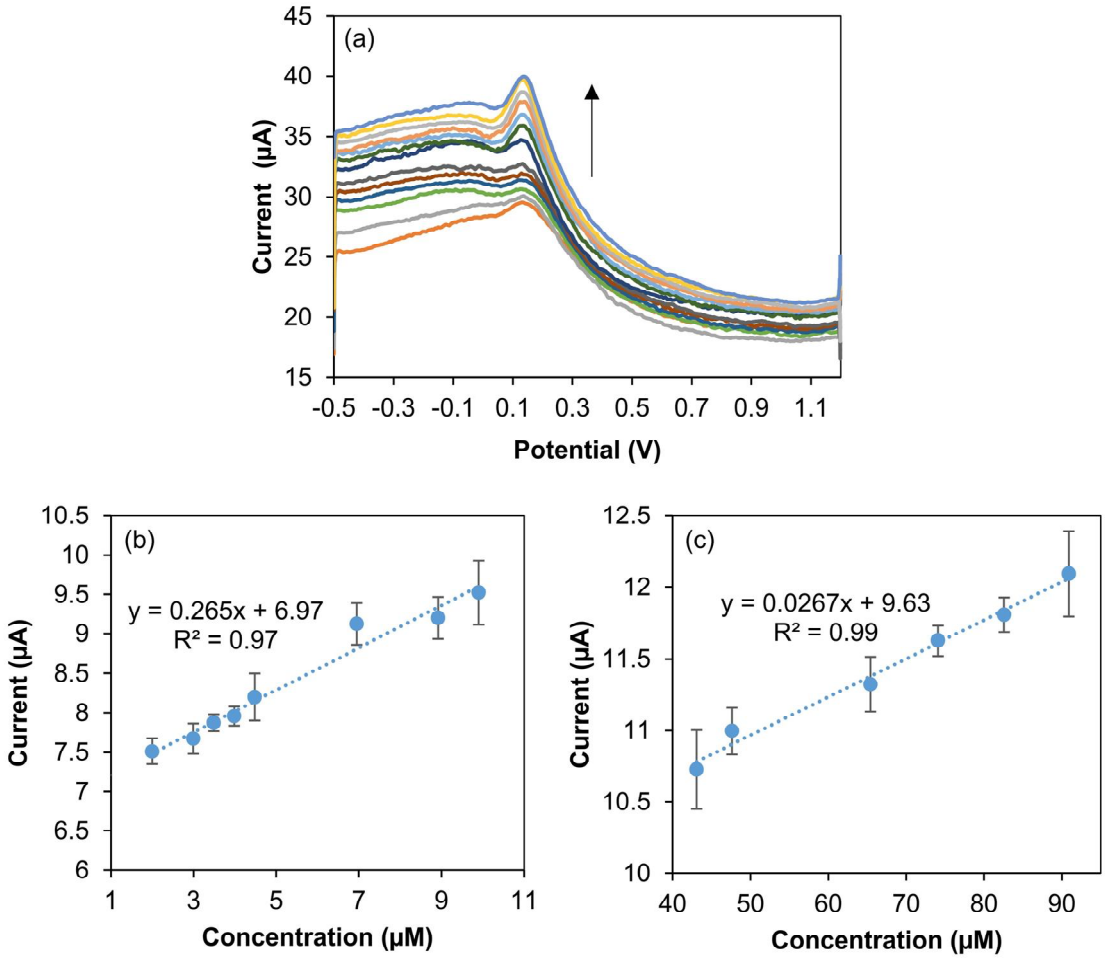

Fig. 8. DPV of MOCP-GrCOOH-Lac/GCE biosensor (a), HQ calibration curve for MOCP-GrCOOH-Lac in different HQ concentrations in the range of (b) 2.0-9.9 µM, and (c) 43.06-90.9 at the scan rate of 0.1 V s^{-1}.

Table 3. Comparable Methods for Determination of Hydroquinone

Biosensor	Linear range (μM)	LOD (μM)	Sensitivity (μA/μM)	Ref.
MOCP-GrCOOH-Lac/GCE	2.0-9.9 43.06-90.9	1.70	0.265 0.0267	This work
Lac/AuNPs/GNPls/SPCE	4-130	1.5	0.0029	[57]
Lac/AP-rGOs/Chit/GCE	3-2000	2	0.01416	[58]
TiO_2/CuCNFs/Lac/GCE	1-89.9	3.65	0.0246	[59]
PANI/MG-Lac-GCE	0.4-337.2	2.94	0.03647	[60]

Gold nanoparticles/graphene nanoplatelets-modified screen-printed carbon electrode (Lac/AuNP/GNPl/SPCE); 1-aminopyrene (1-AP) functionalized reduced graphene oxides (rGOs); chitosan (Chit); TiO_2 loaded copper and carbon composite nanofibers (TiO_2/CuCNFs); polyaniline/magnetic graphene (PANI/MG).

Table 4. Determination of HQ Content in Tap Water Samples

Sample	Real value (μM)	Detection value (μM)	Mean recovery (%)	RSD (%) (n = 3)
1	4.98	4.93	99.08	3.12
2	26.29	23.96	91.15	6.08
3	58.38	54.30	93.01	6.01

Calibration Curve and Detection Limit of MOCP-GrCOOH-Lac Biosensor

Figure 8a illustrates the calibration curve and DPV obtained in different concentrations for the detection of HQ in PB (0.1 M, pH 6) at the potential range of -0.5 to 1.2 V. Figures 8b and 8c demonstrate the relationship between the anodic current of the biosensor and the HQ concentrations by DPV technique. It was found two linear ranges of 2.0-9.9 μM and 43.06-90.9 μM with the correlation coefficients of R^2 equal to 0.97 and 0.99, respectively, and a detection limit of 1.70.

In Table 3, the performance of the biosensor presented here is compared to that of the other Lac biosensors. Accordingly, the limit of detection of our biosensor for HQ detection is comparable to other biosensors.

The proposed biosensor demonstrated a high sensitivity and an acceptable performance because of the synergistic catalytic effect of MOCP and GrCOOH nanosheets, indicating that the synthesized structure for Lac immobilization could help to increase this biosensor detection performance.

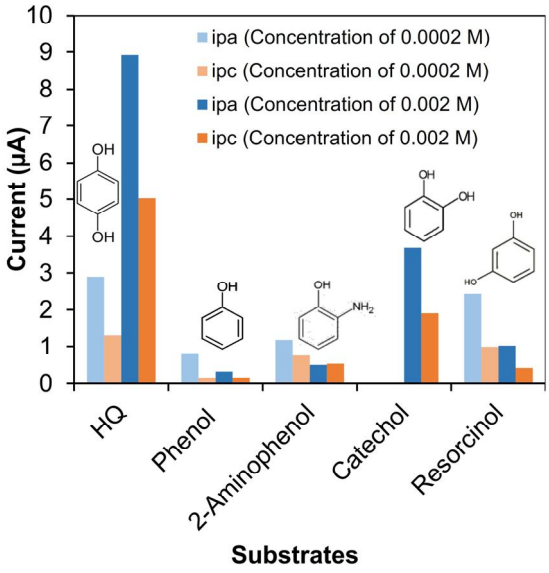

Fig. 9. Voltametric responses of some representative phenols and related compounds using MOCP-GrCOOH-Lac in PB (pH 6) at the same concentrations (0.002 and 0.0002 M); at potential range of -0.5 to 1.2 V.

Determination of HQ Content in Tap Water Samples

The proposed biosensor was used for the detection of HQ in real samples of diluted laboratory tap water using PB of pH 6. The unknown HQ values were estimated from the linear relationship between the current and the concentration indicated in Figs. 8b and 8c. The recoveries (the percentage of the measured value to the real quantity; Table 4) calculated showed that the recoveries of the biosensor are satisfactory and can be employed to find HQ in real samples.

Repeatability, Reproducibility and Stability

To determine the biosensor reproducibility, three electrodes were applied for the preparation of the biosensor presented here. The relative standard deviation (RSD) was figured out to be 6.14%, displaying the acceptable determination of reproducibility for the biosensor. Furthermore, the proposed repeatability of the biosensor was calculated; for doing that, three succeeding current signals were listed and the RSD was estimated to be 2.9%, which is a reasonable value. Also, the steadiness of the fabricated biosensor was evaluated; the stability of 95.16% was attained after one week.

Interference Study

Figure 9 exhibits the interference test of MOCP-GrCOOH-Lac/GCE. Interfering substances, similar to HQ structure, were added to PB pH 6.0 and compared. Two concentrations of each phenolic compound were tested. It should be noticed that in these two concentrations, the current responses to HQ were remarkable, and noticeable changes of redox currents in response to HQ were observed compared to the other phenolic compounds. Furthermore, the current responses to the lower concentration of HQ were also more than those to the higher concentration (with the ratio of 10) of other compounds. It indicates that the MOCP-GrCOOH-Lac/GCE has an outstanding catalytic effectiveness and selectivity for HQ.

CONCLUSIONS

In this study, a novel Lac immobilization method was studied using the MOCP-GrCOOH composite through entrapment method. Based on the chemical features of HQ and the multipurpose catalytic characteristics of Lac

along with the electrochemical properties of GrCOOH and MOCP, we successfully established a unique electrochemical approach for the selective determination of HQ using MOCP-GrCOOH-Lac/GCE. The characterizations of the fabricated electrode have done by SEM images, FTIR spectroscopy and voltammetry techniques. FTIR demonstrated the successful synthesis of MOCP and SEM images demonstrated the entrapment of Lac onto MOCP-GrCOOH. The presence of GrCOOH showed an increase in catalytic reaction of redox probe. The resulted data of two linear ranges for MOCP-GrCOOH-Lac/GCE were 2.0-9.9 and 43.06-90.9 μM, and a detection limit of 1.70 μM was obtained.

A quasi-reversible electrochemical reaction process occurs on the proposed modified electrode surface in the presence of HQ and two protons and 2 electrons can participate in the reaction. Furthermore, this biosensor demonstrated acceptable recoveries in real water samples and showed a good stability for one week.

REFERENCES

[1] J.-M. Moon, N. Thapliyal, K.K. Hussain, R.N. Goyal, Y.-B. Shim, Biosens. Bioelectron. 102 (2018) 540.

[2] D. O'Hare, Biosensors and Sensor Systems, Body Sensor Networks, Springer 2014, pp. 55-115.

[3] C.S. Dzah, Y. Duan, H. Zhang, C. Wen, J. Zhang, G. Chen, H. Ma, Food Biosci. (2020) 100547.

[4] S. Malinowski, C. Wardak, J. Jaroszyńska-Wolińska, P.A.F. Herbert, K. Pietrzak, J. Water Process. Eng. 34 (2020) 101150.

[5] S.A.R. Albayati, S. Kashanian, M. Nazari, S. Rezaei, Bull. Mater. Sci. 42 (2019) 187.

[6] M.M. Rodríguez-Delgado, G.S. Alemán-Nava, J.M. Rodríguez-Delgado, G. Dieck-Assad, S.O. Martínez-Chapa, D. Barceló, R. Parra, Trends Analyt Chem. TrAC 74 (2015) 21.

[7] J. Quinchia, D. Echeverri, A.F. Cruz-Pacheco, M.E. Maldonado, J. Orozco, Micromachines 11 (2020) 411.

[8] F.A. Abd Manan, W.W. Hong, J. Abdullah, N.A. Yusof, I. Ahmad, Mater. Sci. Eng. C 99 (2019) 37.

[9] Y. Wee, S. Park, Y.H. Kwon, Y. Ju, K.-M. Yeon, J. Kim, Biosens. Bioelectron. 132 (2019) 279.

[10] J.R. Camargo, M. Baccarin, P.A. Raymundo-Pereira, A.M. Campos, G.G. Oliveira, O. Fatibello-Filho, O.N. Oliveira Jr, B.C. Janegitz, Anal. Chim. Acta 1034 (2018) 137.

[11] A. Kaffash, K. Rostami, H.R. Zare, Enzyme Microb. Technol. 121 (2019) 23.

[12] C. Wu, Z. Liu, H. Sun, X. Wang, P. Xu, Biosens. Bioelectron. 79 (2016) 843.

[13] Y. Zheng, D. Wang, Z. Li, X. Sun, T. Gao, G. Zhou, Colloids Surf. A Physicochem. Eng. Asp. 538 (2018) 202.

[14] S.K. Patel, M.Z. Anwar, A. Kumar, S.V. Otari, R.T. Pagolu, S.-Y. Kim, I.-W. Kim, J.-K. Lee, Biochem. Eng. J. 132 (2018) 1.

[15] S. Palanisamy, S.K. Ramaraj, S.-M. Chen, T.C. Yang, P. Yi-Fan, T.-W. Chen, V. Velusamy, S. Selvam, Sci. Rep. 7 (2017) 1.

[16] N. Maleki, S. Kashanian, M. Nazari, N. Shahabadi, Appl. Biochem. Biotechnol. 66 (2019) 502.

[17] M. Nazari, S. Kashanian, N. Maleki, N. Shahabadi, Bull. Mater. Sci. 42 (2019) 51.

[18] N. Maleki, S. Kashanian, E. Maleki, M. Nazari, Biochem. Eng. J. 128 (2017) 1.

[19] M. Nazari, S. Kashanian, R. Rafipour, Spectrochim Acta A Mol. Biomol. Spectrosc. 145 (2015) 130.

[20] J. Su, J. Fu, Q. Wang, C. Silva, A. Cavaco-Paulo, Crit. Rev. Biotechnol. 38 (2018) 294.

[21] Z. Li, Z. Chen, Q. Zhu, J. Song, S. Li, X. Liu, J. Hazard. Mater. 399 (2020) 123088.

[22] A.N. Yadav, S. Singh, S. Mishra, A. Gupta, Recent Advancement in White Biotechnology Through Fungi, 2019.

[23] R. Hilgers, J.-P. Vincken, H. Gruppen, M.A. Kabel, ACS Sustain. Chem. Eng. 6 (2018) 2037.

[24] J. Liu, Y. Xie, C. Peng, G. Yu, J. Zhou, J. Phys. Chem. B 121 (2017) 10610.

[25] Y. Jia, Y. Chen, J. Luo, Y. Hu, Ecotoxicol. Environ. Saf. 184 (2019) 109670.

[26] E. Wu, Y. Li, Q. Huang, Z. Yang, A. Wei, Q. Hu, Chemosphere 233 (2019) 327.

[27] F. Lassouane, H. Aït-Amar, S. Amrani, S. Rodriguez-Couto, Bioresour. Technol. 271 (2019) 360.

[28] Z. Fathali, S. Rezaei, M.A. Faramarzi, M. Habibi-Rezaei, Int. J. Biol. Macromol. 122 (2019) 359.
[29] S. HajKacem, S. Galai, F.J.H. Fernandez, A.P. de los Ríos, I. Smaali, J.Q. Medina, Appl. Biochem. Biotechnol. 190 (2020) 1.
[30] R. Sarma, M.S. Islam, A.-F. Miller, D. Bhattacharyya, Appl. Mater. Interfaces. 9 (2017) 14858.
[31] V. Semerdzhieva, R. Raykova, D. Marinkova, S. Yaneva, G. Chernev, J. Biosens. Bioelectron. 9 (2018) 2.
[32] J. Gill, V. Orsat, S. Kermasha, Process Biochem. 65 (2018) 55.
[33] J.K. Gill, V. Orsat, S. Kermasha, J. Sol-Gel Sci. Technol. 85 (2018) 657.
[34] M. Lepore, M. Portaccio, Appl. Biochem. Biotechnol. 64 (2017) 782.
[35] L.G. Mohtar, P. Aranda, G.A. Messina, M.A. Nazareno, S.V. Pereira, J. Raba, F.A. Bertolino, Microchem. J. 144 (2019) 13.
[36] Y. Zhang, X. Li, D. Li, Q. Wei, Colloids Surf. B 186 (2020) 110683.
[37] K. Biradha, A. Ramanan, J.J. Vittal, Cryst. Growth Des. 9 (2009) 2969.
[38] H. Yang, X. Qi, X. Wang, X. Wang, Q. Wang, P. Qi, Z. Wang, X. Xu, Y. Fu, S. Yao, Anal. Chim. Acta 1005 (2018) 27.
[39] X. Xu, X. Qi, X. Wang, X. Wang, Q. Wang, H. Yang, Y. Fu, S. Yao, Electrochem. Commun. 79 (2017) 18.
[40] M.Y. Masoomi, A. Morsali, Coord. Chem. Rev. 256 (2012) 2921.
[41] X. Li, H. Wang, Y. Shimizu, A. Pyatenko, K. Kawaguchi, N. Koshizaki, Chem. Commun. 47 (2010) 932.
[42] S.-L. Hu, K.-Y. Niu, J. Sun, J. Yang, N.-Q. Zhao, X.-W. Du, J. Mater. Chem. A 19 (2009) 484.
[43] M. Bottini, C. Balasubramanian, M.I. Dawson, A. Bergamaschi, S. Bellucci, T. Mustelin, J. Phys. Chem. B 110 (2006) 831.
[44] Y.Y. Yilmaz, E.E. Yalcinkaya, D.O. Demirkol, S. Timur, Sens. Actuators B Chem. 307 (2020) 127665.
[45] E.P. Cipolatti, A. Valerio, R.O. Henriques, D.E. Moritz, J.L. Ninow, D.M. Freire, E.A. Manoel, R. Fernandez-Lafuente, D. de Oliveira, RSC Adv. 6 (2016) 104675.
[46] G. Dai, Z. Li, F. Luo, S. Ai, B. Chen, Q. Wang, Microchim. Acta 186 (2019) 620.
[47] S. Desai, C. Nityanand, Asian J. Biotechnol. 3 (2011) 98.
[48] J.-M. Bollag, A. Leonowicz, Appl. Environ. Microbiol. 48 (1984) 849.
[49] M.S. Ferreira, A.F. Silva Filho, V.L. Martins, M.M. Andrade, D.A. Giarola, L.H. Dall'Antonia, Acta Sci., Technol. 37 (2015) 265.
[50] J.E. Otto, University of South Florida, 2005.
[51] A.J. Bard, L.R. Faulkner, Electrochemical Methods 2 (2001) 580.
[52] M. Haghighi, M. Shahlaei, M. Irandoust, A. Hassanpour, New and Sensitive Sensor for Voltammetry Determination of Methamphetamine in Biological Samples.
[53] H.M. Nassef, A.-E. Radi, C. O'Sullivan, Anal. Chim. Acta 583 (2007) 182.
[54] R. Rafipour, S. Kashanian, F.A. Tarighat, Anal. Chim. Acta 8 (2014) 196.
[55] M. Klis, J. Rogalski, R. Bilewicz, Bioelectrochemistry 71 (2007) 2.
[56] Y. Zhang, Z. Lv, J. Zhou, Y. Fang, H. Wu, F. Xin, W. Zhang, J. Ma, N. Xu, A. He, Electroanalysis 32 (2020) 142.
[57] I. Zrinski, K. Pungjunun, S. Martinez, J. Zavašnik, D. Stanković, K. Kalcher, E. Mehmeti, Microchem. J. 152 (2020) 104282.
[58] X.-H. Zhou, L.-H. Liu, X. Bai, H.-C. Shi, Sens. Actuators B Chem. 181 (2013) 661.
[59] J. Yang, D. Li, J. Fu, F. Huang, Q. Wei, J. Electroanal. Chem. 766 (2016) 16.
[60] C. Lou, T. Jing, J. Zhou, J. Tian, Y. Zheng, C. Wang, Z. Zhao, J. Lin, H. Liu, C. Zhao, Int. J. Biol. Macromol. 149 (2020) 1130.